

Detection of A Novel Reactive Metabolite of Diclofenac: Evidence for
CYP2C9-mediated Bioactivation via Arene Oxides

Zhengyin Yan, Jian Li, Norman Huebert, Gary W. Caldwell, Yanming Du, Hua Zhong

Division of Drug Discovery

Johnson & Johnson Pharmaceutical Research & Development, LLC

Spring House, PA 19477

(Revised, DMD/2004/003095)

Running title: Cytochrome P450 2C9-mediated Bioactivation of Diclofenac

Corresponding Author:

Zhengyin Yan
Drug Discovery
R2013
Johnson & Johnson Pharmaceutical Research & Development, LLC
Welsh & McKean Roads
Spring House, PA 19477-0779

Tel. (215)-628-5036
Fax: (215)-628-7064
E-mail: zyan@prdus.jnj.com

Number of:

Text Page (with references): 29
References: 34
Schemes: 4
Tables: 2
Figures: 7
Supplemental figures: 3

Word count:

Abstract: 249
Introduction: 513
Discussion: 1600

Abbreviations:

COX, cyclooxygenase; CYP, cytochrome P450; UGT: uridine diphosphate
glucuronosferase; GSH, glutathione; HLM, human liver microsomes; MLM:
monkey liver microsomes; RLM: rat liver microsomes; MS, mass spectrometry;
CID: collision induced dissociation; NL: neutral loss MS scan.

Abstract

A new glutathione adduct (**M4**) was tentatively identified, likely as 2'-hydroxy-3'-(glutathione-S-yl)-monoclofenac, using LC-MS/MS analysis of incubations of diclofenac with human liver microsomes. The same conjugate was not detected in incubations with either rat or monkey liver microsomes. Formation of **M4** was mediated specifically by CYP2C9 in human liver microsomes, as evidenced by the following observations: 1, cDNA-expressed CYP2C9 catalyzing formation of **M4**; 2, inhibition of **M4** formation by sulfaphenazole, a CYP2C9-selective inhibitor; 3, strong correlation between the production of **M4** and CYP2C9-mediated tolbutamide 4-hydroxylase activities in a panel of human liver microsome samples. Formation of **M4** suggests the existence of a new reactive intermediate as diclofenac-2', 3'-oxide. A tentative pathway states that diclofenac is oxidized to diclofenac-2', 3'-oxide that reacts with GSH to form a thioether conjugate at the C-3' position, followed by a concomitant loss of chlorine to give rise of **M4**. Furthermore, a likely mechanism leading to the formation of diclofenac oxides is rationalized: CYP2C9 catalyzed oxidation at the C-3' position of the dichlorophenyl ring to form a cationic σ -complex that subsequently results in diclofenac-3', 4'-oxide and diclofenac-2', 3'-oxide; the former oxide is converted to 4'-OH-diclofenac as a major metabolite and can be trapped by GSH to produce 4'-hydroxy-3'-glutathione-S-yl diclofenac (**M2**), whereas the latter oxide forms 3'-OH-diclofenac and can be trapped by GSH to produce **M4**. This mechanism is consistent with the structural modeling of the CYP2C9-diclofenac complex, which reveals that both the C-3' and C-4' of the dichlorophenyl ring are proximate to the heme group.

Introduction

Diclofenac is a nonsteroidal anti-inflammatory drug that is widely prescribed for the treatment of osteoarthritis, rheumatoid arthritis, ankylosing spondylitis and acute muscle pain conditions (Small, 1989). Presumably, pharmacological efficacy of diclofenac is produced from inhibition of cyclooxygenases (COXs). Treatment with diclofenac has been associated with a rare, but severe, incidence of hepatic injury (Banks, et al., 1995; Boelsterli, 2003), which is often described as idiosyncratic toxicity. Although the exact mechanism of diclofenac hepatotoxicity is not clearly understood, it has been proposed that metabolic activation of the drug and subsequent covalent modifications of host proteins by reactive metabolites may play an important role, either by directly impairing cellular signal transduction cascades or indirectly eliciting an immune response, as modified proteins can be recognized as foreign antigens by host cells (Boelsterli, 2003).

As shown in Scheme 1, diclofenac contains a dichlorophenyl ring and a phenyl acetic acid moiety. In humans, metabolism of diclofenac is mediated by both glucuronidation and oxidative biotransformation (Tang, 2003). Glucuronidation of the carboxylic acid group is catalyzed by uridine diphosphate glucuronosyltransferase 2B7 (UGTs) (King, et al., 2001); formed diclofenac-1-*O*-acyl glucuronide has been shown to be chemically reactive and covalently binds to cellular proteins via glycation and/or transacylation (Kretz-Rommel, et al., 1994a; Kretz-Rommel, et al., 1994b). Oxidation of the aromatic rings of diclofenac is mediated by cytochrome P-450s (CYPs). As seen in Scheme 1, hydroxylation of the dichlorophenyl ring is catalyzed specifically by CYP2C9 to produce 4'-hydroxydiclofenac as the major metabolite (Leemann, et al., 1993). At

higher drug concentrations, CYP3A4-mediated oxidation of the phenyl acetic acid moiety results in 5-hydroxydiclofenac (Shen, et al., 1997a). In rat bile after dosing with diclofenac, three glutathione adducts have been previously identified (Tang, et al., 1999a) as 5-hydroxy-4-glutathione-S-yl diclofenac (**M1**), 4'-hydroxy-3'-glutathione-S-yl diclofenac (**M2**) and 5-hydroxy-6-glutathione-S-yl diclofenac (**M3**). Subsequent in-vitro studies have shown that both 4'-hydroxydiclofenac and 5-hydroxydiclofenac could be further oxidized to benzoquinone imine intermediates that were trapped as GSH adducts **M1-3**, respectively (Tang, et al., 1999a). These observations have led to a two-step bioactivation mechanism: 1, diclofenac is first converted to 4'-hydroxydiclofenac and 5-hydroxydiclofenac via direct hydroxylation; 2, these two metabolites are further oxidized to form benzoquinone imine intermediates by CYP2C9 and CYP3A4, respectively (Scheme 1) (Tang, et al., 1999a; Tang, et al., 1999b). These findings are significant as the first line of evidence to suggest that CYP-mediated reactive metabolites may play an important role in toxicity of the drug.

Although several protein adducts have been detected in rats treated with diclofenac (Jones, et al., 2003; Shen, et al., 1997b), the relationship between covalent modifications and diclofenac hepatotoxicity has not been clearly established (Tang, 2003). Characterization of reactive metabolites would be very helpful for understanding biochemical mechanisms of idiosyncratic toxicity associated with diclofenac. In this study, we report a novel reactive metabolite in the form of a glutathione adduct in NADPH-fortified human liver microsomes incubated with diclofenac; in addition, it was found that formation of the reactive metabolite was specifically mediated by CYP2C9.

These data are important for further understanding the relationship between metabolic activation of diclofenac and the hepatotoxicity of the drug observed in clinic.

Materials and Methods

Materials.

Reagents and solvents used in the current study were of the highest possible grade available. The following chemicals were purchased from Sigma-Aldrich (St. Louis, MO), including acetaminophen, 1-aminobenzotriazole (ABT), dextromethorphan, dextrorphan, diclofenac, glutathione, 4'-hydroxy-diclofenac, ketoconazole, α -naphthoflavone, phenacetin, testosterone, 6 β -hydroxy-testosterone, tolbutamide, sulphaphenazole, tranlycypromine, quinidine, trichloroacetic acid, β -nicotinamide adenine dinucleotide phosphate (NADP⁺), glucose-6-phosphate and glucose-6-phosphate dehydrogenase. All microsomes, including rat and monkey liver microsomes, *Supersomes* containing cDNA-expressed CYPs, pooled and individually prepared human liver microsomes, were obtained from Gentest Corp. (Woburn, MA). (*S*)-mephenytoin, 4'-hydroxy-mephenytoin and 4-hydroxy-tolbutamide were all supplied by *Ultrafine* Chemicals (Manchester, UK). Stable-isotope labeled glutathione [GSX, γ -glutamyl-cystein-glycin-¹³C₂-¹⁵N] was obtained from Cambridge Isotope Laboratories (Andover, MA), and isotopic purity was 94% estimated by the supplier using NMR. Acetonitrile and methanol were from EMD Chemicals (Gibbstown, NJ).

Instruments.

MS analyses were performed on a Micromass (Manchester, UK) *Quattro Micro* triple quadrupole mass spectrometer that was interfaced to an Agilent 1100 HPLC system (Agilent Technologies, Palo Alto, CA). The ESI ion source was operated in the positive

ion mode, and experimental parameters were set as follows: capillary voltage 3.2 kV, source temperature 120 °C, desolvation temperature 300 °C, sample cone voltage 26 V. Data were processed using the *Masslynx* version 4.0 software from Micromass.

NMR spectrum of the diclofenac derivative was obtained on a Bruker 300 NMR spectrometer, and chemical shifts were expressed relative to tetramethylsilane.

Microsomal Incubations.

All incubations were performed at 37°C in a water bath. Diclofenac or its derivative was individually mixed with human, monkey or rat liver microsomal protein in 50 mM potassium phosphate buffer (pH 7.4) supplemented with glutathione. After a 5-min preincubation at 37°C, reactions were initiated by the addition of a NADPH generating system to give a final volume of 1.0 mL. The final reaction mixture contained 10 µM drug compound, 1 mg/mL microsomal protein, 1 mM GSH or GSX, 1.3 mM NADP⁺, 3.3 mM glucose-6-phosphate, 0.4 U/mL glucose-6-phosphate dehydrogenase and 3.3 mM magnesium chloride. After a 60-min incubation, reactions were terminated by the addition of 150 µL of trichloroacetic acid (10%). Incubations with recombinant CYP enzymes were performed similarly, except that liver microsomes were substituted by *Supersomes*. Samples were centrifuged at 10000 g for 15 min at 4 °C to pellet the precipitated protein, and supernatants were subjected to LC-MS/MS for direct analysis of GSH adducts. For the neutral loss MS/MS scanning of GSH adducts, supernatants were concentrated by solid phase extraction as described below, prior to LC-MS/MS analyses.

Inhibition of CYPs by Chemical Inhibitors.

The effect of specific inhibitors of individual CYP enzymes on the formation of reactive metabolites was investigated using pooled human liver microsomes. Reaction mixtures contained diclofenac, individual CYP specific inhibitors, GSH and microsomal proteins. Reactions were initiated by the addition of the NADPH regenerating solution. The final concentration of microsomal protein was 1 mg/mL. Incubations proceeded for 20 min, and reactions were terminated by the addition of trichloroacetic acid. CYP selective inhibitors, α -naphthoflavone (1 μ M), sulfaphenazole (5 μ M), tranilcypromine (12.5 μ M), quinidine (2 μ M) and ketoconazole (1 μ M), were used to investigate the involvement of CYP1A2, CYP2C9, CYP2C19, CYP2D6 and CYP3A4, respectively. In the control, no chemical inhibitors were included in incubations. Duplicate incubations were performed for each CYP inhibitor.

The effectiveness of individual CYP inhibitors was evaluated using pooled human liver microsomes incubated with CYP marker substrates, as previously described (Yan, et al. 2002). Compounds used as CYP marker substrates were 10 μ M phenacetin (CYP1A2), 100 μ M (*S*)-mephenytoin (CYP2C19), 500 μ M tolbutamide (CYP2C9), 80 μ M dextromethorphan (CYP2D6), and 150 μ M testosterone (CYP3A4). Individual marker substrates were preincubated with human liver microsomes in the presence and absence of CYP-selective inhibitors for 5 min at 37 °C prior to the addition of a NADPH generating solution. After incubation for 20 min, reactions were terminated, and metabolites generated from individual CYP marker substrates were analyzed by the LC-MS/MS method (Yan, et al. 2002). A comparison was made relative to the controls (no inhibitors), and activity was expressed as the percentage of control activity remaining.

Correlation with marker substrate activities.

A panel of 12 human livers was used to assess the formation of reactive metabolites of diclofenac. Microsomes prepared from these livers had been previously characterized for individual CYP marker activities by the supplier (Gentest Corp., Woburn, MA). Marker substrates used to determine specific CYP activities were phenacetin (CYP1A2), coumarin (CYP2A6), (*S*)-mephenytoin (CYP2C19 and CYP2B6), paclitaxel (CYP2C8), diclofenac (CYP2C9), bufuralol (CYP2D6), chlorzoxazone (CYP2E1), testosterone (CYP3A4) and lauric acid (CYP4A). Because diclofenac is the subject of this study, CYP2C9 activity was internally re-evaluated using tolbutamide as a marker substrate, and a good correlation (r 0.92) was found between 4-hydroxy-tolbutamide activity and 4'-hydroxy-diclofenac activity among the panel of 12 liver microsomal preparations.

A correlation study was conducted between the formation of reactive metabolites and enzymatic activities of specific CYP isozymes across the entire human liver microsome panel, under the same incubation conditions.

Synthesis of 2'-Hydroxymonoclofenac.

A total amount of 200 mg diclofenac was dissolved in 4 mL NaOH (3 M), and supplemented with 2 mL of DMF. The diclofenac solution was transferred to a 10 mL CEM reaction vial containing a magnetic stirring bar. The reaction vial was properly sealed and degassed under vacuum, and then subjected to microwave irradiation for 60 min on a CEM Discovery Microwave Apparatus operated at 200 °C and the power level of 150 W. The crude reaction mixture was concentrated by lyophilizing, and the residue was separated by flash chromatography on reverse phase silica gel (gradient elution, H₂O

: CH₃CN from 1 : 0 to 1 : 1) to provide 2-hydroxymonoclofenac. After lyophilizing, 50 mg of the product was obtained as a white solid. High resolution MS (MH⁺) *m/z*: 278.0571 (calcd: 278.0584) measured by Micromass LCT. ¹H NMR (300 MHz, CDCl₃) δ 7.56-7.50 (m, 2H), 7.44-7.34 (m, 2H), 7.23(t, *J* = 7.8 Hz, 1H), 7.12 (t, *J* = 7.5 Hz, 1H), 6.42 (d, *J* = 7.7 Hz, 1H), 3.80 (s, 2H).

Solid-phase Extractions.

Samples resulting from incubations were desalted and concentrated by solid-phase extraction (SPE), prior to neutral loss scan MS/MS analyses. SPE was performed using SEP-PAK cartridges packed with 100 mg of sorbent C₁₈ (Waters Corp., Milford, MA). Cartridges were first conditioned with 5 mL methanol, and then flushed with 5 mL of water. Samples resulting from centrifugation were loaded into cartridges, and cartridges were washed with 5 mL of water to remove salts and proteins. Components of interest were eluted from cartridges with 1 mL of methanol. Eluted components were dried on a SpeedVac dryer. The dried samples were resuspended in 150 μL of water-acetonitrile (95:5), and were then subjected to neutral loss scan MS/MS analyses.

LC-MS/MS Analyses.

For complete profiling of reactive metabolites, samples were first subjected to chromatographic separations with an Agilent 1100 HPLC system integrated with an auto-sampler (Agilent Technologies, Palo Alto, CA), and eluents were introduced to the *Quattro Micro* triple quadrupole mass spectrometer that was operated in the neutral loss scanning mode as described above. An Agilent Zorbax SB C18 column (2.1 x 150 mm) was used for chromatographic separations. The starting mobile phase consisted of 95% water (0.5% acetic acid), and the metabolites were eluted using a single gradient of 95%

water to 85% acetonitrile over 25 min at a flow rate of 0.3 mL/min. At 25 min, the column was flushed with 85% acetonitrile for 2 min before re-equilibration at initial conditions. LC-MS/MS analyses were carried out on 10- μ L aliquots of cleaned samples. Mass spectra collected in the neutral loss scanning mode were obtained by scanning over the range m/z 400-700 in 2s. After a positive peak was detected, a CID MS/MS spectrum was subsequently obtained to further elucidate the structure of the glutathione conjugate.

For relative comparison of GSH adduct levels, the mass spectrometer was operated in the multiple reaction monitoring (MRM) mode. Three transitions were simultaneously monitored in detecting **M1-3**, including m/z 617 \rightarrow 542, 617 \rightarrow 488, and 617 \rightarrow 342, and transitions used for detecting **M4** are m/z 583 \rightarrow 508, 583 \rightarrow 454 and 583 \rightarrow 308.

Molecular Modeling.

Superimposition of the structures of CYP2C9-warfarin complex (PDB code: 1OG5) (Williams et al., 2003) and CYP2C5-diclofenac complex (PDB code: 1NR6) (Wester, et al., 2003) revealed that the heme active sites for CYP2C5 and CYP2C9 are nearly identical, except for a few residues in CYP2C9 warfarin binding site which are specific for CYP2C9. We assumed that diclofenac binds to CYP2C9 in a similar conformation as in CYP2C5. Accordingly, the CYP2C9-diclofenac complex structure was constructed by a molecular docking procedure using CYP2C5-diclofenac complex crystal structure as a reference: 1OG5 and 1NR6 structures were first overlaid; the bound warfarin was removed from 1NR6 structure to obtain the apo-1NR6 protein structure, diclofenac conformation in 1OG5 was subsequently copied to apo-1NR6 structure as a reference molecule. Then, Schrodinger Glide software (Maestro 6.0, Schrodinger, Inc.,

Portland, OR) was used to dock a free diclofenac to the apo-1NR6 structure guided by the reference 1OG5 diclofenac conformation. The energy of the best-scoring pose was then fully minimized using Schrodinger Maestro with OPLS-AA force field (Kaminski, et al., 2001).

Results

Characterization of the GSH Adducts Formed in Microsomal Incubations.

Previous clinical studies (Degen, et al., 1988; Davies, et al., 1997) have indicated that peak concentrations (*C_{max}*) of diclofenac are in the range of 1-17 μM in human plasma after a single dose of 100 mg given orally. To be clinically relevant, 10 μM of diclofenac was used in all incubations performed in this study.

For the initial screening of GSH adducts, samples generated from incubations with human liver microsomes were desalted and concentrated by solid phase extractions, and resulting samples were subjected to LC/MS/MS neutral loss scan detecting ions that lost both 129 and 75 Da upon collision induced dissociation (CID) (Baillie, et al., 1993). As shown in Figure 1, two major components that exhibited response to both neutral losses (129 and 75 Da) were detected at retention times of 13.2 (component **I**) and 13.6 min (component **II**) respectively in incubations of diclofenac with human liver microsomes. The peak area ratio of **I** to **II** was approximately 1.0 for the neutral loss scan of 129 Da and 0.7 for the neutral loss scan of 75 Da, respectively. Neither **I** or **II** was detected when either diclofenac or the NADPH regenerating system was omitted from incubations. Additionally, formation of both **I** and **II** was abated by pre-incubation of HLM with 15 μM ABT for 15 min in the presence of NADPH generating system (data

not shown). These results suggested that GSH adducts were formed from a reactive metabolite of diclofenac via CYP-mediated oxidation.

The parent ion of component **I** at retention time 13.3 min was at m/z 583 (Figure **2a** and **2b**). A chlorine isotope peak was observed at m/z 585 (~ 37% of the M+1 ion), which clearly indicated the formation of a new GSH adduct that contained only one chlorine atom. Subsequent CID MS/MS spectrum of the MH^+ at m/z 583 gave product ions at m/z 508 and 454, resulting from neutral losses of glycine (75 Da) and γ -glutamate (129 Da), respectively, which confirmed the presence of a GSH moiety in the metabolite (Figure **3**). A GSH adduct, either 2'-hydroxy-3'-(glutathione-S-yl)-monoclofenac or 3'-hydroxy-2'-(glutathione-S-yl)-monoclofenac, was tentatively proposed, which is consistent with the chlorine isotope cluster and cleavage of CID product ions. The plausible fragmentation pathways are shown in Scheme **2**. The molecular ions of the GSH adduct underwent a loss of water to give rise of ions at m/z 565; double cleavages at the α -carbon of glycine formed product ions at m/z 334, and cleavage adjacent to the thioether moiety led to the product ion at m/z 308 that subsequently lost a water to form ions at m/z 290; a further loss of CO from ions at m/z 290 gave rise of m/z 262. Product ions at m/z 508 and at m/z 454 resulting from the neutral losses underwent a further loss of water to form ions at m/z 490 and m/z 436, respectively; a loss of NH_3 from ions at m/z 436 resulted in product ions at m/z 419. The newly identified GSH adduct was assigned as **M4** in this study, following **M1-3** previously identified by others (Tang, et al., 1999a).

The parent ion associated with component **II** at retention time 13.6 min was at m/z 617 with a chlorine isotope peak at m/z 619 (~ 75% of the M+1 ion) (**S1**), suggesting that this component was one of the three GSH adducts previously identified (Tang, et al.,

1999a). This was confirmed by the CID spectrum of the MH^+ ions at m/z 617 that existed product ions at m/z 599, 542, 488, 470, 342 and 324. Component **II** was subsequently identified as **M2** by comparing the retention time of the GSH adduct formed by 4'-hydroxydiclofenac incubated with CYP2C9 (Tang, et al., 1999b).

Stable Isotope Labeling of GSH Adducts in Microsomal Incubations.

To further verify the identity of GSH adducts, GSX, a triply labeled glutathione (two C^{13} and one N^{15} at glycine), was used to trap reactive metabolites generated in human liver microsomal incubations (Yan, et al., 2004). Neutral loss scanning MS analyses of samples generated from HLM incubations revealed a mass shift of 3 Da for molecular ions of both **M4** (m/z 586) and **M2** (m/z 620), respectively. Additionally, stable isotope labeled **M4** and **M2** displayed identical chlorine isotope clusters of their natural counterparts. Tandem MS spectrum of **M4** at m/z 586 is shown in Figure 4. As expected, product ions at m/z 508, 490, 334, 308, 290 and 262 were detected; new product ions at m/z 457, 439 and 422 appeared, which apparently correspond to product ions at m/z 454, 436 and 419 of unlabeled **M4** (Figure 3).

GSH Conjugate Formation in Human, Monkey and Rat Liver Microsomes.

LC-MS/MS was used to detect GSH adducts **M1-4** formed in incubations of diclofenac with human, monkey and rat liver microsomes. Interestingly, **M4** was detected only in the incubation with human liver microsomes (Figure 5). Species difference was also found for **M1-3**. **M2** was the most abundant GSH conjugate formed in human liver microsomes; small amounts of **M1** were detected in the incubation with monkey liver microsomes; both **M1** and **M3** were detected in incubations with rat liver microsomes, and the former conjugate is more predominant (**S2**).

GSH Adduct Formation in Incubations with Recombinant CYPs.

The formation of the GSH adducts was investigated in microsomes derived from insect cell expressed recombinant human CYP1A2, CYP2C8, CYP2C9, CYP2C19, CYP2D6, CYP2E1 and CYP3A4. As seen in Figure 6, at the same enzyme concentration (100 pmoles/mL), CYP2C9 generated the most amount of **M4**; although CYP2C19 also catalyzed **M4** formation, the level of **M4** was less than 2% of that formed by CYP2C9. No **M4** was detected in incubations with other CYP enzymes including CYP1A2, CYP2C8, CYP2D6, CYP2E1 and CYP3A4.

GSH adduct **M2** was also detected in the same incubations. It was found that, consistent with observations by others (Tang, et al., 1999b), formation of **M2** was specifically mediated by CYP2C9, and no **M2** was detected in incubations with other CYPs including CYP2C19 (**S3**). **M1** and **M3** were primarily derived from CYP3A4-mediated oxidation of the phenyl acetic acid ring, and thus were not the focus of this study.

Inhibition of CYP-Mediated Diclofenac Bioactivation.

The inhibitory effect of specific inhibitors of individual CYP enzymes on the formation of **M2** and **M4** was examined using pooled human liver microsomes. Since the concentration of inhibitors used in the inhibition study varied widely among different laboratories, the effective concentrations were determined in house using pooled human liver microsomes and CYP marker substrates (Yan, et al., 2002). The formation of both **M2** and **M4** was strongly inhibited (> 70%) by the CYP2C9 selective inhibitor sulphaphenazole (5 μ M) in human liver microsomal incubations (Table 1). However, the inhibitory effect on **M2** and **M4** formation was minimal (< 10%) for other CYP selective

inhibitors including α -naphthoflavone (CYP1A2), tranlycypromine (CYP2C19), quinidine (CYP2D6) and ketoconazole (CYP3A4), although significant inhibition (> 60%) by these selective inhibitors was observed in the metabolism of corresponding CYP marker substrates (Table 1).

Formation of M2 and M4 in a Panel of Human Liver Microsomes.

Studies were carried out to investigate the correlation between formation of **M2** and **M4** and enzymatic activities of individual CYP enzymes (1A2, 2A6, 2B6, 2C8, 2C9, 2C19, 2D6, 2E1 and 3A4). As shown in Table 2, a strong correlation was observed between 4-hydroxy-tolbutamide activity, a CYP2C9 marker activity, and the extent of formation of **M2** (r 0.89, p < 0.005) and **M4** (r 0.84, p < 0.005). Correlations were insignificant between the extent of formation of **M2** and **M4** and the marker activity of other CYPs in the entire panel of human liver microsomes (Table 2).

Structural Modeling of CYP2C9-Diclofenac Complex.

Although a crystal structure of CYP2C9-diclofenac complex has not been reported yet, the recently published structures for CYP2C5-diclofenac complex (Williams, et al., 2003) and CYP2C9-warfarin complex (Wester, et al., 2003) provide excellent templates for modeling CYP2C9-diclofenac complex structure. CYP2C5 and 2C9 share high sequence identity (77%) and similarity (83%), and also exhibit the same regio-selectivity and similar catalytic efficiency for oxidation of diclofenac (Williams, et al., 2003). Therefore, it is reasonable to assume that diclofenac binds to CYP2C9 and CYP2C5 in a very similar bonding mode.

Figure 7 depicts the binding mode of diclofenac in the CYP2C9 heme active site. Similar to what is seen in CYP2C5-diclofenac complex, the phenyl acetic acid ring distal

from the heme group can form π - π interaction with Phe114 and Phe476. Together with the hydrogen bond network formed by the carboxylate group to Asp293 and Asn107, this π - π interaction is the key interaction to anchor the diclofenac in the active site; in agreement with the mutagenesis experiments (Melet, et al., 2003), the structure shows that Phe114 and Phe476 of CYP2C9 are key residues in diclofenac recognition. The dichlorophenyl ring is proximate to heme group, consistent with the fact that the oxidation of diclofenac by CYP2C9 occurs in this part of the molecule. Most noticeably, the orientation of the dichlorophenyl ring places the 3'- carbon atom closest to the heme iron atom, and the distance between Fe and C-3' is 4.4 Å, and C-4' is located 4.7 Å from heme iron atom. This structure clearly suggests that the active high-valent iron-oxo likely attacks both the C-3' and C-4' during the oxidation reaction, since two carbons are close to the oxo atom. Based on the homology modeling, Melet *et al* published a CYP2C9-diclofenac complex structure also revealing that C-3' in the dichlorophenyl ring is in the closest proximity to the heme iron atom (Melet, et al., 2003). It is our current belief that the CYP2C9-diclofenac binding mode in Figure 6 provides a structural rationale for the formation of both **M2** and **M4**.

Discussion

Chemically reactive metabolites have been implicated in the biochemical mechanisms of idiosyncratic toxicity of diclofenac, and great efforts have been made to characterize reactive intermediates formed in rats and in-vitro incubations (Tang, et al., 1999a; Tang, et al., 1999b; Poon, et al., 2001). However, the proof of reactive metabolites as a causative agent for drug related hepatotoxicity still remains elusive

(Tang, 2003). It is essential to completely understand bioactivation pathways of diclofenac in order to address its mechanism of toxicity.

In this study, a new GSH adduct (**M4**) was detected using LC-MS/MS in incubations of diclofenac with human liver microsomes. Glutathione moiety of **M4** was further confirmed by tandem MS spectrum of the stable isotope labeled conjugate that exhibited a mass shift of 3 Da in neutral loss MS scanning. It was also found that **M4** formation is specifically mediated by CYPs. Additionally, it is interesting to observe that **M4** was formed only in incubations with human liver microsomes. This observation may provide a likely explanation for the fact that **M4** was not previously detected in rat bile (Tang, et al., 1999a) after dosing with diclofenac.

Similar to that of **M2**, formation of **M4** in human liver microsomes is mediated specifically by CYP2C9. This conclusion is supported by the following observations: 1, recombinant CYP2C9 catalyzed formation of **M2** and **M4** in incubations; 2, both **M2** and **M4** formation was strongly inhibited by sulfaphenazole, a CYP2C9 selective inhibitor; 3, a strong correlation was observed between **M2** and **M4** formation and CYP2C9 marker activity in a panel of human liver microsomes preparations. CYP2C19, an isoform sharing 88% homology with CYP2C9, also catalyzed the formation of **M4**, but the conversion rate was significantly lower than that of CYP2C9. Therefore, CYP2C19 is unlikely to play a major role in the bioactivation of diclofenac in human liver microsomes. This argument is also supported by the finding that tranlycypromine, a CYP2C19 selective inhibitor, did not inhibit **M4** formation in human liver microsomes, but effectively suppressed (*S*)-mephenytoin 4'-hydroxylation, a CYP2C19 marker activity (Table 1); in addition, **M4** formation was not correlated with CYP2C19 marker

activity as measured by (*S*)-mephenytoin 4'-hydroxylation in a panel of human liver microsomes (Table 2).

A two-step oxidation mechanism has previously been proposed for the bioactivation of the dichlorophenyl ring, direct oxidation at the C-4' position resulting in 4'-hydroxydiclofenac followed by further oxidation to form a benzoquinone imine (Tang, et. al, 1999a). CYP2C9-mediated formation of the new GSH adduct **M4** suggests that an additional metabolism pathway may also be responsible for the bioactivation of diclofenac. Unlike **M2**, **M4** contains one chlorine atom, clearly indicating that CYP-mediated epoxidation between the C-2' and C-3' position of the dichloroaniline ring is the most reasonable mechanism by which a loss of chlorine could result after conjugation with GSH. Two GSH adducts, 2'-hydroxy-3'-(glutathione-S-yl) monoclofenac and 3'-hydroxy-2'-(glutathione-S-yl) monoclofenac, conform the CID MS/MS spectrum of **M4** (Figure 3). Another isomer, 4'-hydroxy-2'-(glutathione-S-yl) monoclofenac, would also give a similar CID MS/MS spectrum, but formation of this isomer requires CYP-mediated oxidation at the C-4' position and substitution of chlorine with glutathione catalyzed by glutathione-S-transferases (GSTs). A separated incubation of 4'-hydroxydiclofenac with NADPH-fortified HLM did not produce **M4** (data not shown), which ruled out the involvement of GSTs in the formation of **M4**. Attempts were made to isolate **M4** directly from incubations of diclofenac with CYP2C9 using preparative LC, but failed to obtain enough amounts of the conjugate in the desired purity for NMR analyses, due to the low abundance of GSH adducts and co-eluting of **M2** and **M4** on preparative columns. Efforts to synthesize **M4** have currently been hampered by lacking a feasible chemistry strategy.

Regardless, formation of **M4** is indicative of a unique reactive metabolite formed by diclofenac. We rationalized a metabolic pathway, in attempt to explain **M4** formation in human liver microsomal incubations. As shown in Scheme 3, diclofenac is first oxidized to diclofenac-2', 3'-oxide that is trapped in incubations as 2'-hydroxy-3'-GS-2', 3'-dihydro-diclofenac; the GSH adduct further undergoes a loss of HCl, resulting in a stable conjugate 2'-hydroxy-3'-(glutathione-S-yl)-monoclofenac. Alternatively, another isomeric adduct could form by conjugating GSH to diclofenac-2', 3'-oxide at the C-2' position, resulting in 3'-hydroxy-2'-GS-2', 3'-dihydrodiclofenac that subsequently lost HCl to form 3'-hydroxy-2'-(glutathione-S-yl)-monoclofenac. However, the C-2' position of the arene oxide would be somewhat sterically hindered by both chlorine and the aniline ring, and thus 3'-hydroxy-2'-(glutathione-S-yl)-monoclofenac was not formed. It is our current speculation that **M4** detected in this study is 2'-hydroxy-3'-(glutathione-S-yl)-monoclofenac. Obviously, it is highly desirable to further confirm the proposed structure using a synthetic compound.

Considering the fact that hydroxylation of diclofenac-2', 3'-oxide would result in 3'-hydroxydiclofenac, this mechanism is in agreement with the following observations: 1, 3'-hydroxydiclofenac was detected in human after dosing with diclofenac (Stierlin, et al., 1979; Sawchuk, et al., 1995); 2, similar to that of **M2**, formation of 3'-hydroxydiclofenac is mediated specifically by CYP2C9 in human liver microsomes (Bort, et al., 1999).

Another likely pathway is that CYP2C9 mediates ipso substitution of chlorine to form a phenol metabolite that is further oxidized to a benzoquinone imine. This intermediate also conjugates with GSH to produce **M4**. To investigate this potential bioactivation mechanism, the proposed phenol metabolite, 2'-hydroxymonoclofenac, was

chemically synthesized. However, **M4** was not detected in incubations of 2'-hydroxydiclofenac with either human liver microsomes or recombinant CYP2C9 (data not shown).

CYP450-mediated epoxidation reactions represent a common biotransformation pathway for aromatic hydroxylation (Guengerich, 2002). Several aromatic compounds such as bromobenzene (Jollow, et al., 1974) and lamotrigine (Maggs, et al., 2000) are metabolized by CYPs via forming reactive arene oxides. Although the exact mechanism leading to formation of arene oxides has not been completely understood yet, many kinetic and theoretical studies of benzene hydroxylation by CYP enzymes support a model in which a cationic σ -complex (or radical σ -complex) is first produced, prior to the formation of arene oxides (Ortiz de Montellano, 1995; de Visser, et al., 2003). As diclofenac-3', 4'-oxide has previously been proposed to be the precursor molecule of 4'-hydroxydiclofenac (Blum, et al., 1996) and whose formation was mediated specifically by CYP2C9 (Leemann, et al., 1993), we hypothesized that both diclofenac-3', 4'-oxide and diclofenac-2', 3'-oxide are formed via a common intermediate. As depicted in Scheme 4, oxidation at the 3'-C position of diclofenac generates a cationic σ -complex (or radical σ -complex) that subsequently forms two isomeric oxides, diclofenac-3', 4'-oxide and diclofenac-2', 3'-oxide. Because the NH is a strong para-directing group, diclofenac-3', 4'-oxide is converted to 4'-OH-diclofenac as the major metabolite. Also, 3', 4'-oxide conjugates with GSH to form **M2**. It should be noted that formed 4'-OH-diclofenac can be further oxidized to a benzoquinone imine that can be trapped by GSH as **M2** (Tang, et al, 1999a). Similarly, diclofenac-2', 3'-oxide forms 3'-OH-diclofenac and can be trapped as **M4** in the presence of GSH. This epoxidation mechanism is supported by the

structure of CYP2C9-diclofenac complex, which was constructed using crystal structures of CYP2C5-diclofenac complex (Williams, et al., 2003) and CYP2C9-warfarin complex (Wester, et al., 2003) as our modeling templates. As seen in Figure 6, the C-3' is proximate to the heme iron and in a favorable position for CYP2C9-mediated oxidation. Because of high homology between CYP2C9 and 2C5, the structure of CYP2C9-diclofenac complex is considered to be highly reliable. In addition, this structure is consistent with modeling results reported by others (Melet, et al., 2003).

In the two-step bioactivation model (Tang, et al., 1999a), a direct hydroxylation occurs at C-4' position to give rise of 4'-hydroxydiclofenac as the major metabolite. This mechanism is also supported by the structure of CYP2C9-diclofenac complex which reveals that the C-4' is close to the heme group. However, the two-step mechanism alone could not elaborate the formation of 3'-OH-diclofenac and **M4** in incubations of diclofenac with CYP2C9. The two-step model is primarily substantiated by the finding that CYP2C9 catalyzed oxidation of 4'-OH-diclofenac to form **M2** in incubations in the presence of GSH (Tang, et al., 1999a). However, conversion of 4'-OH-diclofenac to **M2** is not conclusive evidence to suggest that 4'-OH-diclofenac is an obligatory intermediate for the formation of **M2** from diclofenac.

In this study, we proposed epoxidation as an additional mechanism leading to the bioactivation of diclofenac, in an attempt to provide a likely explanation for the formation of 3'-OH-diclofenac and 4'-OH-diclofenac, **M2** and **M4** in the presence of GSH. It is likely that both mechanisms, direct hydroxylation at the C'-4 and epoxidation at the C'2-C3' (Scheme 4), are responsible for the bioactivation of diclofenac, given the fact that

both the C-4' and C'-3 are proximate to the heme, and 4'-OH-diclofenac is a major metabolite that can be further oxidized to diclofenac-1', 4'-quinone imine.

In conclusion, a novel reactive intermediate was detected in incubations of diclofenac with human liver microsomes. Consistent with formation of the glutathione adduct, a bioactivation pathway leading to the formation of diclofenac-2', 3'-arene oxide is rationalized. The precursor of 2'-hydroxy-3'-(glutathione-S-yl)clofenac was proposed to be diclofenac-2', 3'-arene oxide whose formation is specifically mediated by CYP2C9. It is our hypothesis that, in addition to the two-step mechanism proposed by others (Tang, et al., 1999a), bioactivation of diclofenac occurs at the C-3' position, resulting in 3', 4-oxide and 2', 3'-oxide respectively. Given the fact that arene oxides are known causative agents in the toxicity of many toxicants (Guengerich, 2001), identification of diclofenac arene oxides further substantiates the speculation that oxidative bioactivation may play a significant role in the toxicity of diclofenac. Considering the association of arene oxides with hepatotoxicity (Guengerich, 2001), the present finding is of significance in understanding the toxicology mechanism of diclofenac, and more mechanistic studies are warranted in the future. One would expect that a crystal structure of CYP2C9-diclofenac complex would provide more conclusive information on this subject.

References

Banks, A. T., Zimmerman, H. J., Ishak, K. G., Harter, J. G. (1995) Diclofenac-associated hepatotoxicity: analysis of 180 cases reported to the food and drug administration as adverse reactions. *Hepatology* **22**, 820-827.

Baillie, T. A., Davis, M. R. (1993) Mass spectrometry in the analysis of glutathione conjugates. *Biol. Mass Spectrom.* **22**, 319-325.

Blum, W., Faigle, J. W., Pfaar, U., Sallmann, A. (1996) Characterization of a novel diclofenac metabolite in human urine by capillary gas chromatography-negative chemical ionization mass spectrometry. *J. Chromatog. B: Biomed. Appl.* **685**, 251-263.

Boelsterli, U. A. (2003) Diclofenac-induced liver injury: a paradigm of idiosyncratic drug toxicity. *Toxicol. Appl. Pharm.* **192**, 307-322.

Bort, R., Mace, K., Boobis, A., Gomez-Lechon, M. J., Pfeifer, A., Castell, J. (1999) Hepatic metabolism of diclofenac: role of human CYP in the minor oxidative pathways. *Biochem. Pharmacol.* **58**, 787-796.

Davies, N. M., Anderson, K. E. (1997) Clinical pharmacokinetics of diclofenac. Therapeutic insights and pitfalls. *Clin. Pharmacokinet.* **33**, 184-213.

Degen, P. H., Dieterle, W., Schneider, W., Theobald, W., Sinterhauf, U. (1988) Pharmacokinetics of diclofenac and five metabolites after single doses in healthy volunteers and after repeated doses in patients. *Xenobiotica* **18**, 1449-1455

de Visser, S. P., Shaik, S. (2003) A proton-shuttle mechanism mediated by the porphyrin in benzene hydroxylation by cytochrome P450 enzymes. *J. Am. Chem. Soc.* **125**, 7413 – 7424.

Guengerich, F. P. (2002) Cytochrome P450 oxidations in the generation of reactive electrophiles: epoxidation and related reactions. *Arch. Biochem. Biophys.* **409**, 59-71.

Guengerich, F. P. (2001) Common and uncommon cytochrome P450 reactions related to metabolism and chemical toxicity. *Chem. Res. Toxicol.* **14**, 611-650.

Jollow, D. J., Mitchell, J. R., Zampaglione, N., Gillette, J. R. (1974) Bromobenzene-induced liver necrosis. Protective role of glutathione and evidence for 3,4-bromobenzene oxide as the hepatotoxic metabolite. *Pharmacology* **11**, 151-69.

Jones, J. A., Kaphalia, L., Treinen-Moslen, M., Liebler, D. C. (2003) Proteomic characterization of metabolites, protein adducts, and biliary proteins in rats exposed to 1,1-dichloroethylene or diclofenac. *Chem. Res. Toxicol.* **16**, 1306-1317.

Kaminski, G. A., Friesner, R. A., Tirado-Rives, J., Jorgensen, W. L. (2001) Evaluation and reparametrization of the OPLS-AA force field for proteins via comparison with accurate quantum chemical calculations on peptides. *J. Phys. Chem. B*, **105**, 6474 – 6487.

King, C., Tang, W., Ngui, J., Tephly, T., Braun, M. (2001) Characterization of rat and human UDP-glucuronosyltransferases responsible for the in vitro glucuronidation of diclofenac. *Toxicol. Sci.* **61**, 49-53.

Kretz-Rommel, A., Boelsterli, U. A. (1994a) Mechanism of covalent adduct formation of diclofenac to rat hepatic microsomal proteins. Retention of the glucuronic acid moiety in the adduct. *Drug Metab. Dispos.* **22**, 956-961.

Kretz-Rommel, A., Boelsterli, U. A. (1994b) Selective protein adducts to membrane proteins in cultured rat hepatocytes exposed to diclofenac: radiochemical and immunochemical analysis. *Mol. Pharmacol.* **45**, 237-244.

Leemann, T., Transon, C., Dayer, P. (1993) Cytochrome P450TB (CYP2C): a major monooxygenase catalyzing diclofenac 4'-hydroxylation in human liver. *Life Sci.* **52**, 29-34.

Maggs, J. L., Naisbitt, D. J.; Tetley, J. N. A., Pirmohamed, M., Park, B. K. (2000) Metabolism of lamotrigine to a reactive arene oxide intermediate. *Chem. Res. Toxicol.* **13**, 1075-1081.

Melet, A., Assris, N., Jean, P., Lopez-Garcia, M. P., Marques-Soares, C., Jaouen, M., Dansette, P. M., Sari, M.-A., Mansuy, D. (2003) Substrate selectivity of human cytochrome P450 2C9: Importance of residues 476, 365 and 114 in recognition of diclofenac and sulfaphenazole and in mechanism-based inactivation by tienilic acid. *Arch. Biochem. Biophys.* **409**, 80-91.

Ortiz de Montellano, P. R. (1995) *Cytochrome P450: Structure, mechanism and biochemistry*, 2nd ed., Plenum Press, New York.

Poon, G. K., Chen, Q., Teffera, Y., Ngui, J. S., Griffin, P. R., Braun, M. P., Doss, G. A., Freeden, C., Stearns, R. A., Evans, D. C., Baillie, T. A., Tang, W. (2001) Bioactivation of diclofenac via benzoquinone imine intermediates-identification of urinary mercapturic acid derivatives in rats and humans. *Drug Metab. Dispos.* **29**, 1608-1613.

Small, R. E. (1989) Diclofenac sodium. *Clinic. Pharm.* **8**, 545-558.

Sawchuk, R. J., Maloney, J. A., Cartier, L. L., Rackley, R. J., Chan, K. K. H., Lau, H. S. L. (1995) Analysis of diclofenac and four of its metabolites in human urine by HPLC. *Pharm. Res.* **12**, 756-762.

Shen, S., Marchick, M. R., Davis, M. R., Doss, G. A., Pohl, L. R. (1997a) 5-Metabolic activation of diclofenac by human cytochrome P450 3A4: role of 5-hydroxydiclofenac. *Chem. Res. Toxicol.* **12**, 214-222.

Shen, S., Hargus, S. J., Martin, B. M., Pohl, L. R. (1997b) Cytochrome P4502C11 is a target of diclofenac covalent binding in rats. *Chem. Res. Toxicol.* **10**, 420-423.

Stierlin, H., Faigle, J. W. (1979) Biotransformation of diclofenac sodium (Voltaren) in animals and in man. II. Quantitative determination of the

unchanged drug and principal phenolic metabolites, in urine and bile.

Xenobiotica. **9**, 611-621.

Stierlin, H., Faigle, J. W., Sallmann, A., Kung, W., Richter, W. J., Kriemler, H. P., Alt, K. O., Winkler, T. (1979) Biotransformation of diclofenac sodium (Voltaren) in animals and in man. I. Isolation and identification of principal metabolites. *Xenobiotica* **9**, 601-610.

Tang, W. (2003) The metabolism of diclofenac--enzymology and toxicology perspectives. *Curr. Drug Metab.* **4**, 319-329.

Tang, W., Stearns, R. A., Bandiera, S. M., Zhang, Y., Raab, C., Braun, M. P., Dean, D. C., Pang, J., Leung, K. H., Doss, G. A., Strauss, J. R., Kwei, G. Y., Rushmore, T. H., Chiu, S. L., Baillie, T. A. (1999a) Studies on cytochrome P-450-mediated bioactivation of diclofenac in rats and in human hepatocytes: identification of glutathione conjugated metabolites. *Drug Metab. Dispos.* **27**, 365-372.

Tang, W., Stearns, R. A., Wang, R. W., Chiu, S. L., Baillie, T. A. (1999b) Roles of human hepatic cytochrome P450s 2C9 and 3A4 in the metabolic activation of diclofenac. *Chem. Res. Toxicol.* **12**, 192-199.

Wester, M. R., Johnson, E. F., Marques-Soares, C., Dijoils, S., Dansette, P. M., Mansuy, D., Stout, D. (2003) Structure of mammalian cytochrome P450 2C5 complexed with diclofenac at 2.1 Å resolution: Evidence for an induced fit model of substrate binding. *Biochemistry* **42**, 9335-9345.

Williams, P. A., Cosme, J., Ward, A., Angove, H., Vinkovic, D. M., Jhoti, H.
(2003) Crystal structure of human cytochrome P450 2C9 with bound warfarin.
Nature **424**, 464-468.

Yan, Z., Caldwell, G. W., Wu, W. N., McKown, L. A., Rafferty, B., Jones, W.,
Masucci, J. A. (2002) In vitro identification of metabolic pathways and
cytochrome P450 enzymes involved in the metabolism of etoperidone.
Xenobiotica **32**, 949-962.

Yan, Z., Caldwell, G. W. (2004) Stable-isotope trapping and high throughput
screenings of reactive metabolites using the isotope MS signature. *Anal. Chem.*
76, 6835-6847.

Legends

- Figure 1.** LC/MS/MS detection of GSH adducts derived from diclofenac by constant scanning for neutral losses of 129 Da (**a**) and 75 Da (**b**).
- Figure 2.** CID-MS/MS spectra of component **I (M4)**. **a**, MS/MS spectrum of neutral loss of 129 Da; **b**, MS/MS spectrum of neutral loss of 75 Da.
- Figure 3.** CID-MS/MS spectra of component **I (M4)** at m/z 583.
- Figure 4.** CID-MS/MS spectra of stable isotope labeled component **I (M4)** at m/z 586.
- Figure 5.** **M4** formation in liver microsomes derived from human (top), monkey (middle) and rat tissues (bottom). Signal responses are normalized in order to compare the level of GSH adduct.
- Figure 6.** Formation of GSH adduct **M4** in incubations with recombinant CYP2C9 (**a**) and CYP2C19 (**b**), respectively. Signal responses are not normalized in order to show **M4** generated by CYP2C19.
- Figure 7.** The modeling structure of CYP2C9-diclofenac complex. Two aromatic rings of diclofenac are in orange, and the heme iron is in purple. Substitutes of diclofenac are shown in green for Cl and blue for the NH group.
- Scheme 1.** Structure of diclofenac and proposed oxidative pathways.
- Scheme 2.** CID Fragmentation pathways of the GSH adduct **M4**.
- Scheme 3.** Proposed the bioactivation pathways leading to the formation of **M4**.

Scheme 4. CYP2C9-mediated oxidation of dichlorophenyl ring of diclofenac via the proposed epoxidation mechanism (solid arrow) and direct hydroxylation pathway (dashed arrow) (Tang, et. al 1999a).

Table 1. Effect of CYP isoform-selective inhibitors on the formation of **M2** and **M4** in HLM incubations.

Inhibitor (CYP), μM	M4 formation ^a	M2 formation ^a	CYP activity ^{a, b}
α -Naphthoflavone (1A2), 1.0	92.4	95.6	17.7
Sulfaphenazole (2C9), 5.0	27.1	29.2	27.7
Tranlycypromine (2C19), 12.5	91.8	91.2	35.6
Quinidine (2D6), 2.0	97.5	104.2	12.4
Ketoconazole (3A4), 1.0	93.5	92.3	18.2

^a, values are the average of duplicates and are expressed as percentages relative to the control (without inhibitors). ^b, CYP activity was determined using known CYP-specific substrates.

Table 2. Correlation between **M2** and **M4** formation and CYP marker activity in HLM.

CYP	Isoform Marker Activity	Correlation Coefficient (r)	
		M4	M2
1A2	Phenacetin O-deethylation	0.11	0.20
2A6	Coumarin 7-hydroxylation	0.05	0.09
2B6	(S)-Mephenytoin N-demethylation	0.21	0.12
2C8	Paclitaxel 6 α -hydroxylation	0.20	0.17
2C9	Tolbutamide 4'-hydroxylation	0.84*	0.89*
2C19	(S)-Mephenytoin 4'-hydroxylation	0.16	0.31
2D6	Bufuralol 1'-hydroxylation	0.09	0.27
2E1	Chlorzoxazone 6-hydroxylation	0.23	0.12
3A4	Testosterone 6 β -hydroxylation	0.31	0.36
4A	Lauric acid 12-hydroxylation	0.18	0.08

* Significantly correlated ($P < 0.005$). Correlation study was carried out using human microsomes prepared from 12 different donors, and represents the average of two determinations.

Figure 1

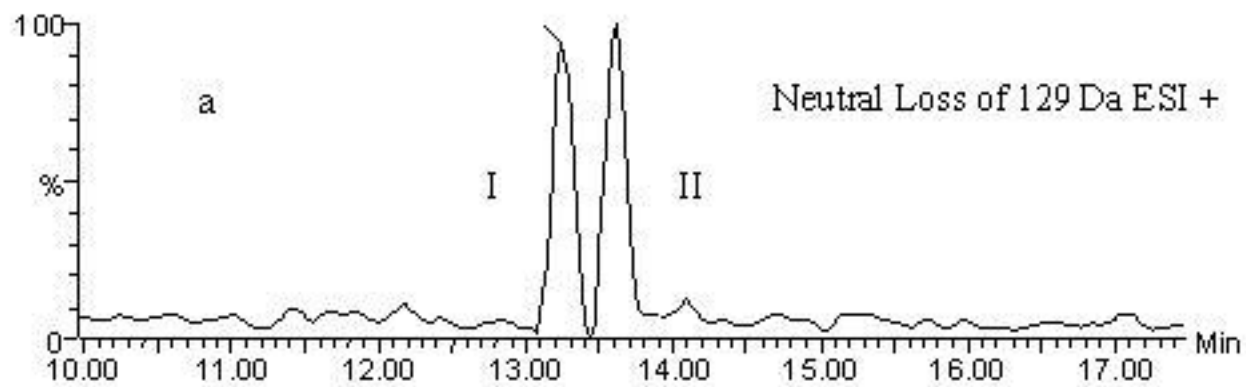
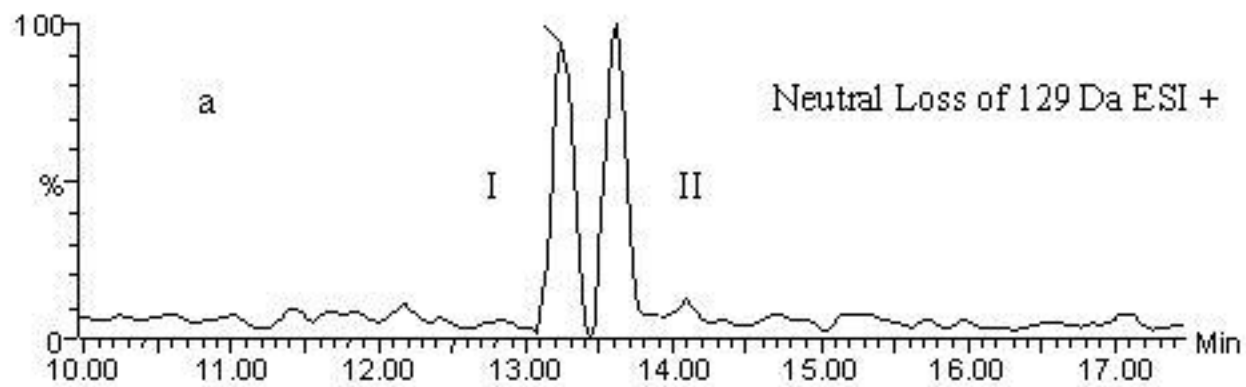


Figure 2

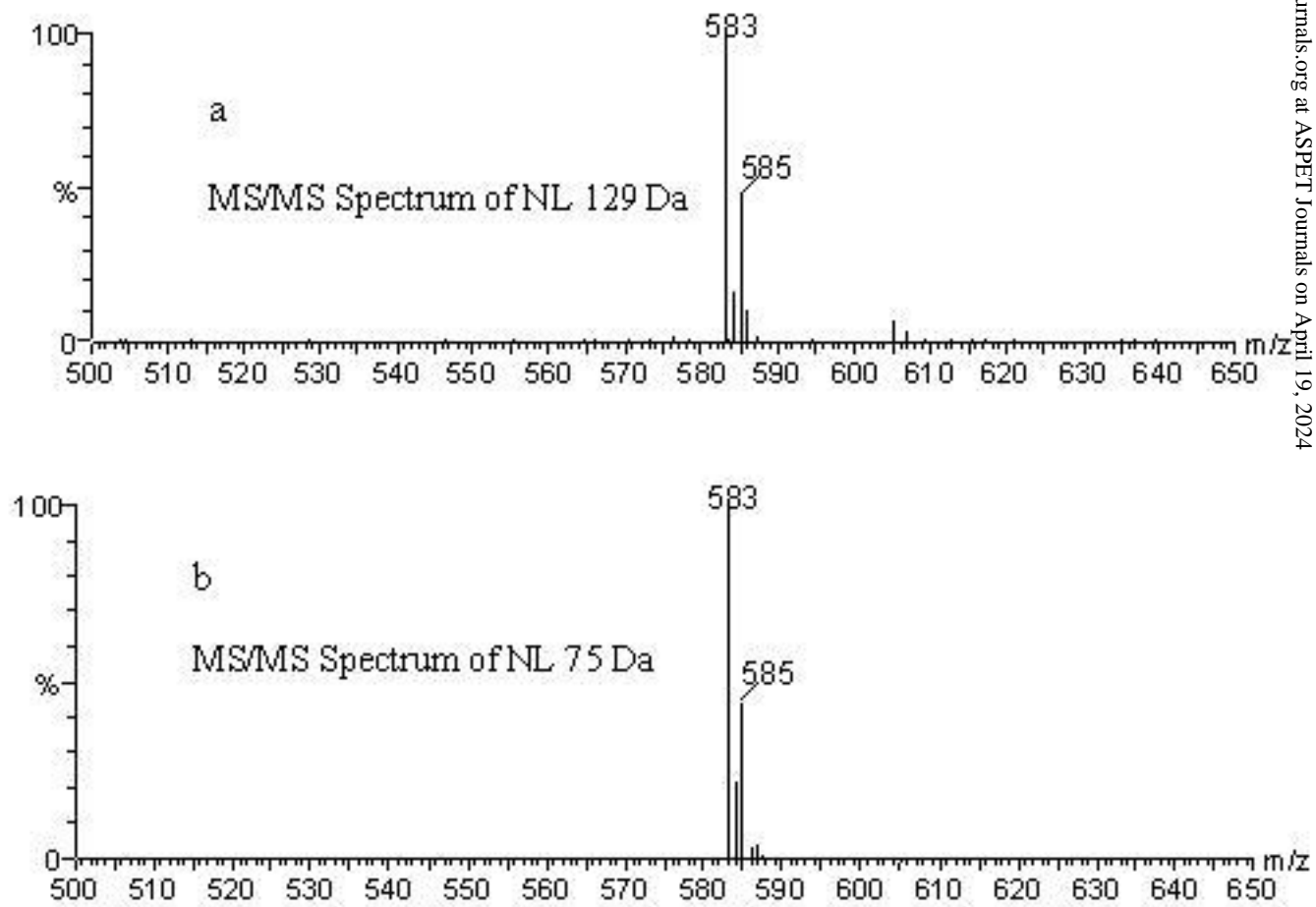


Figure 3

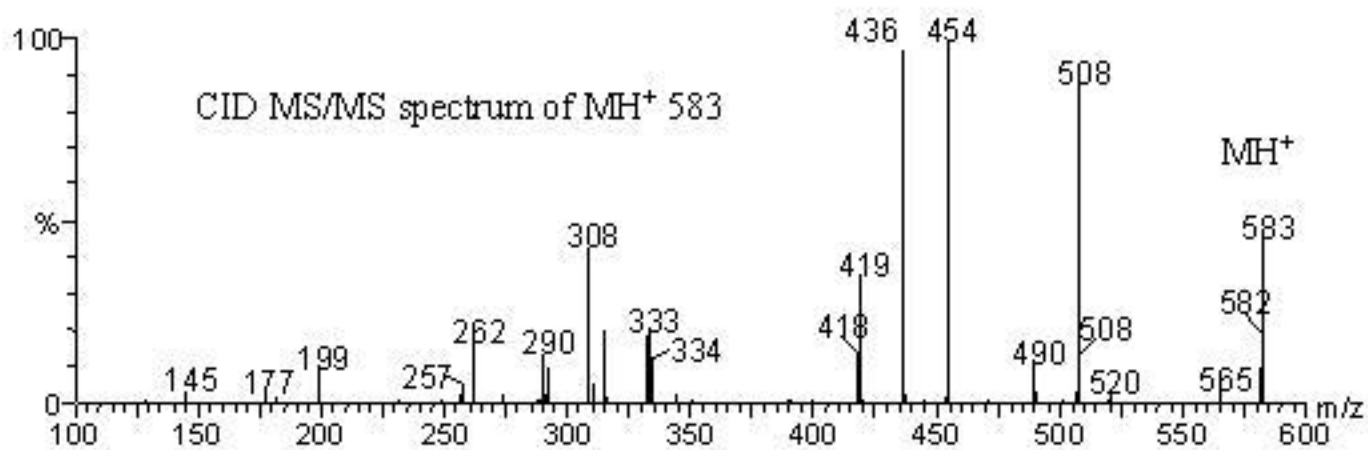


Figure 4

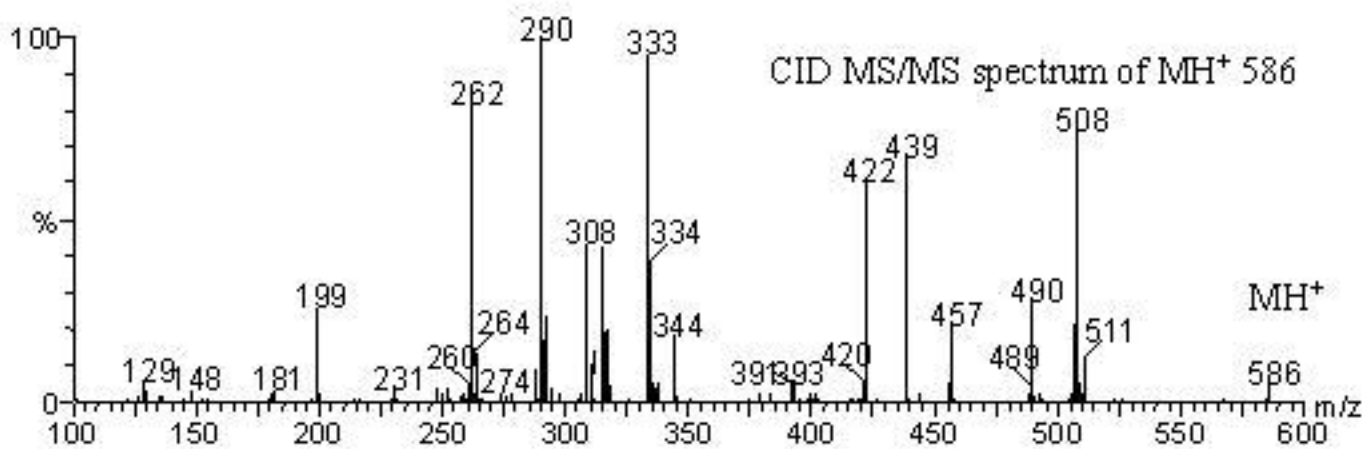
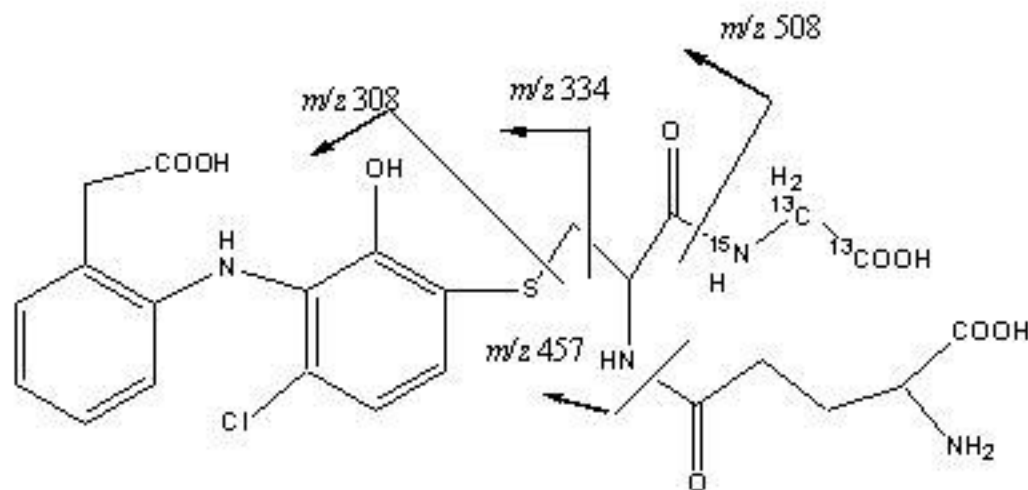


Figure 5

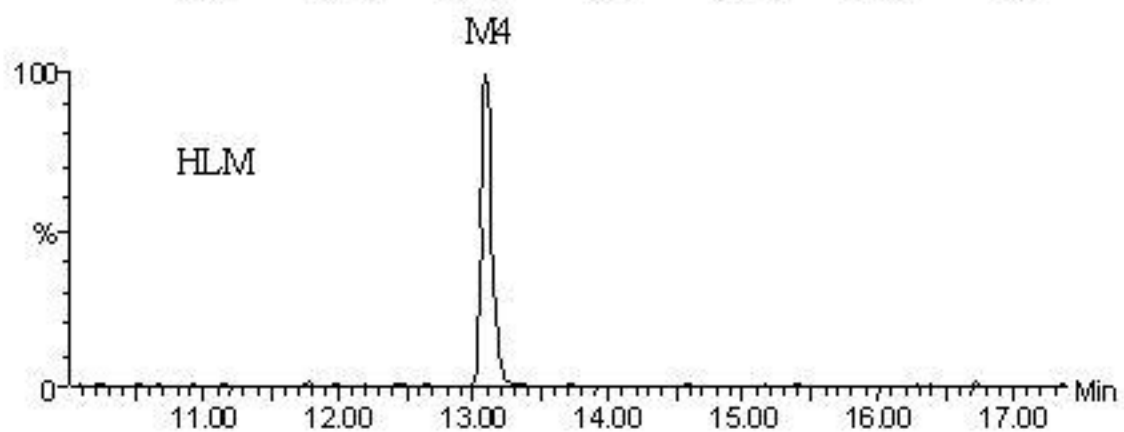
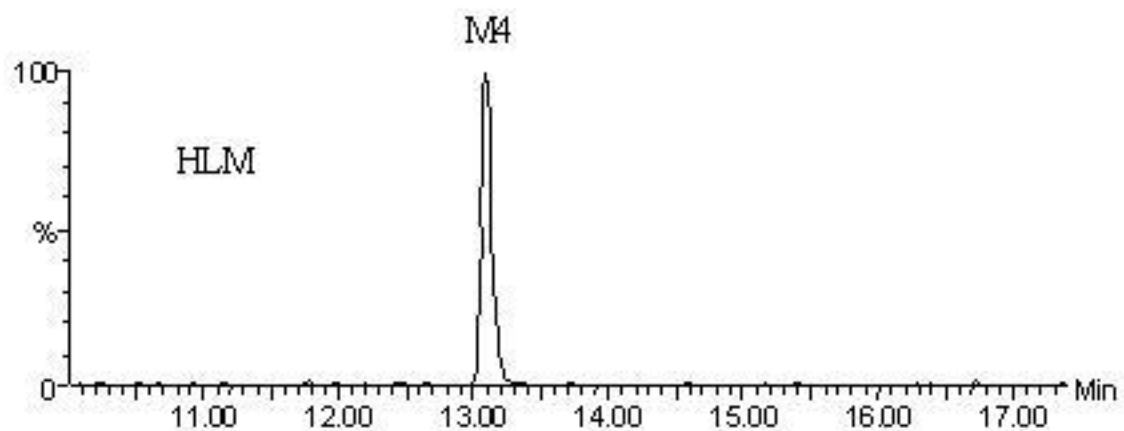
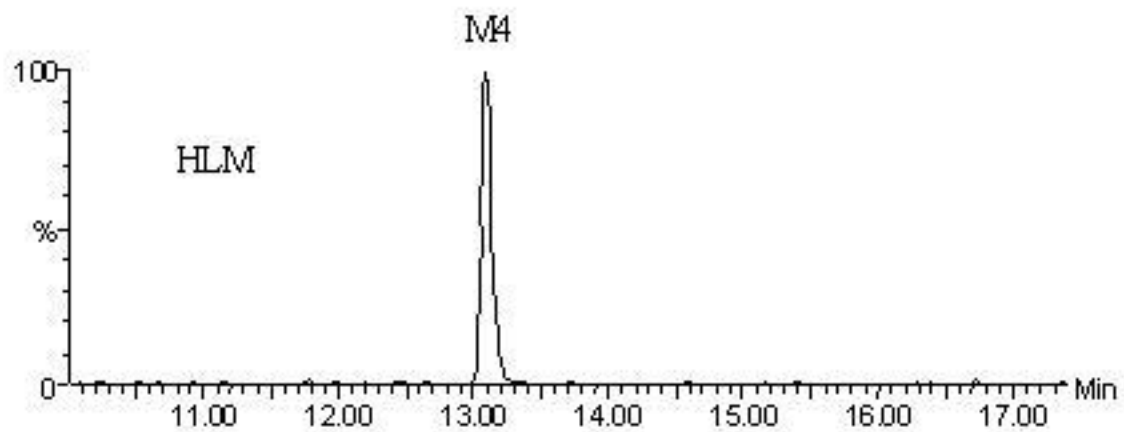


Figure 6

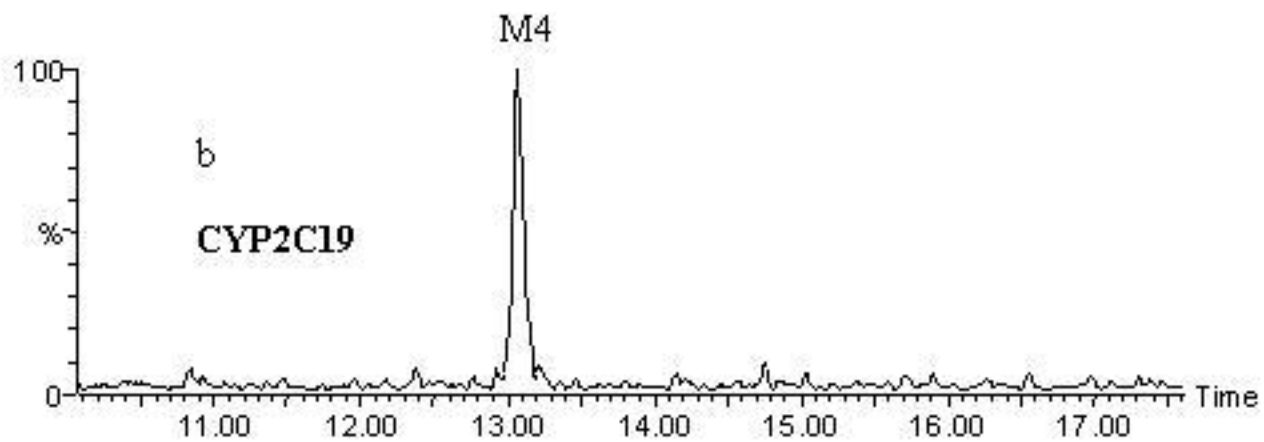
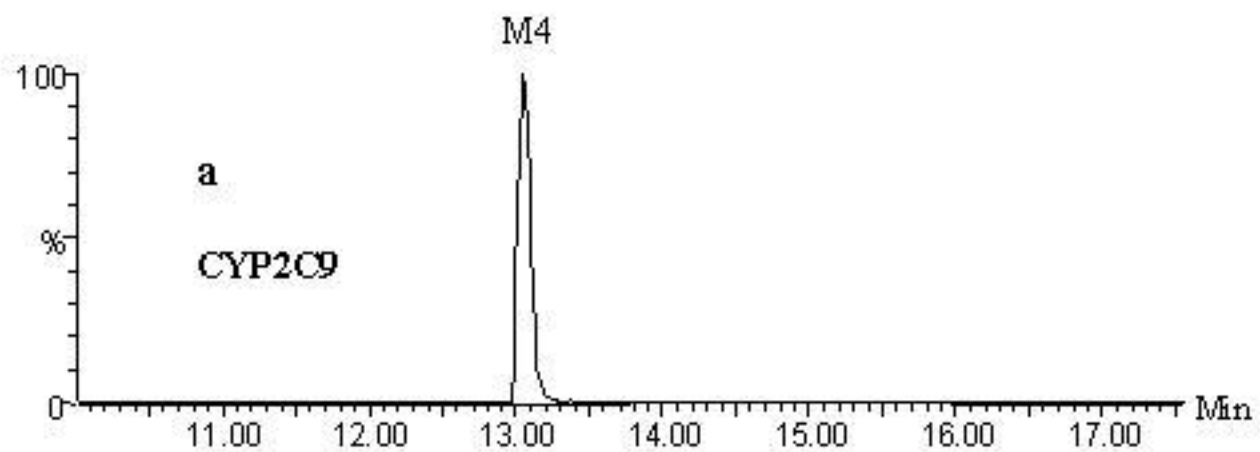
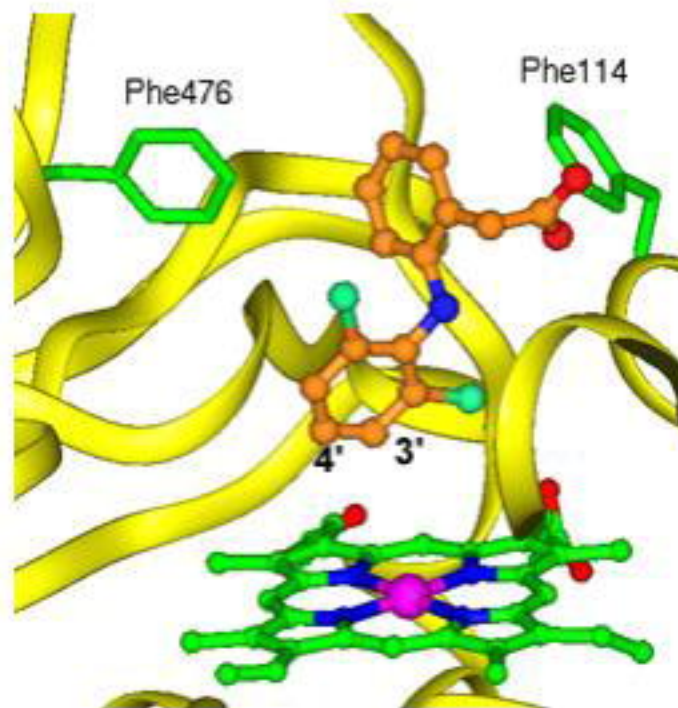
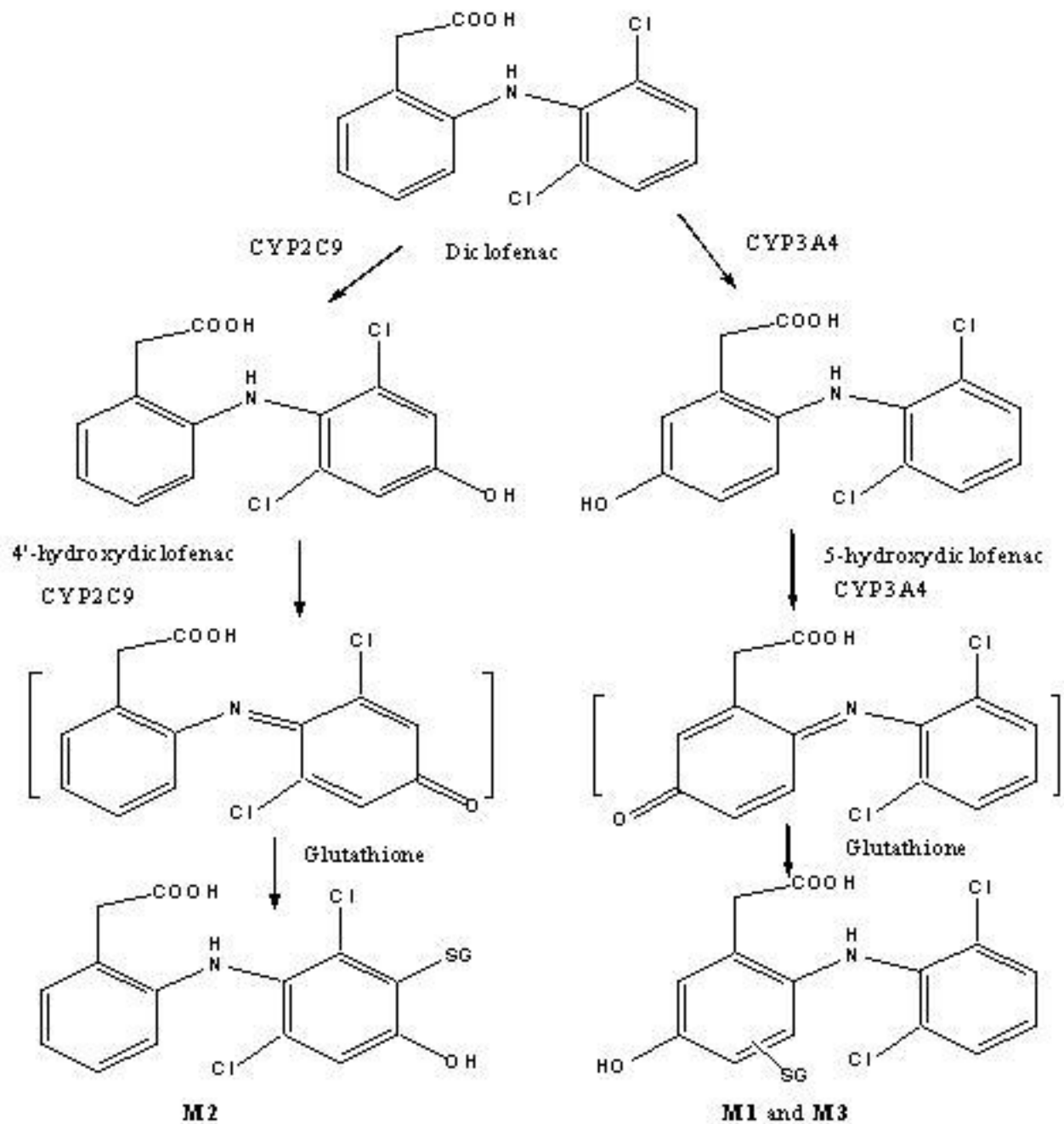


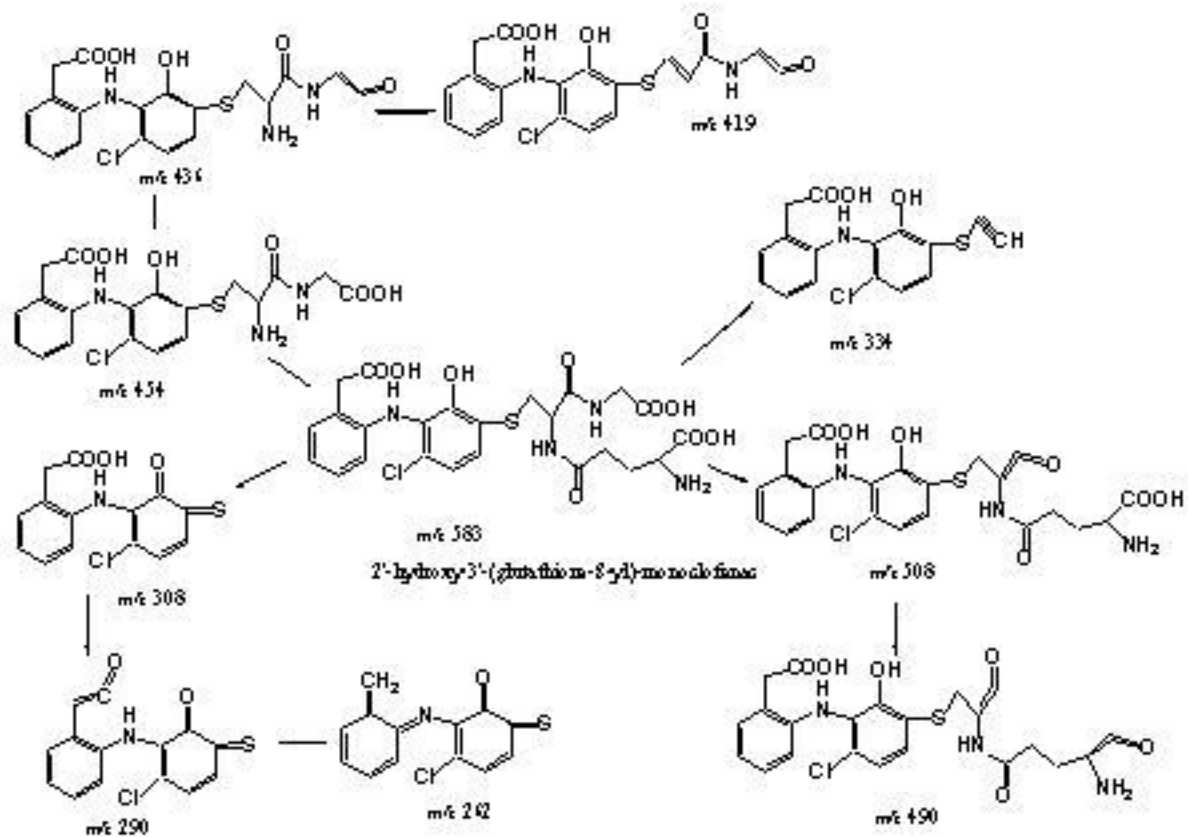
Figure 7



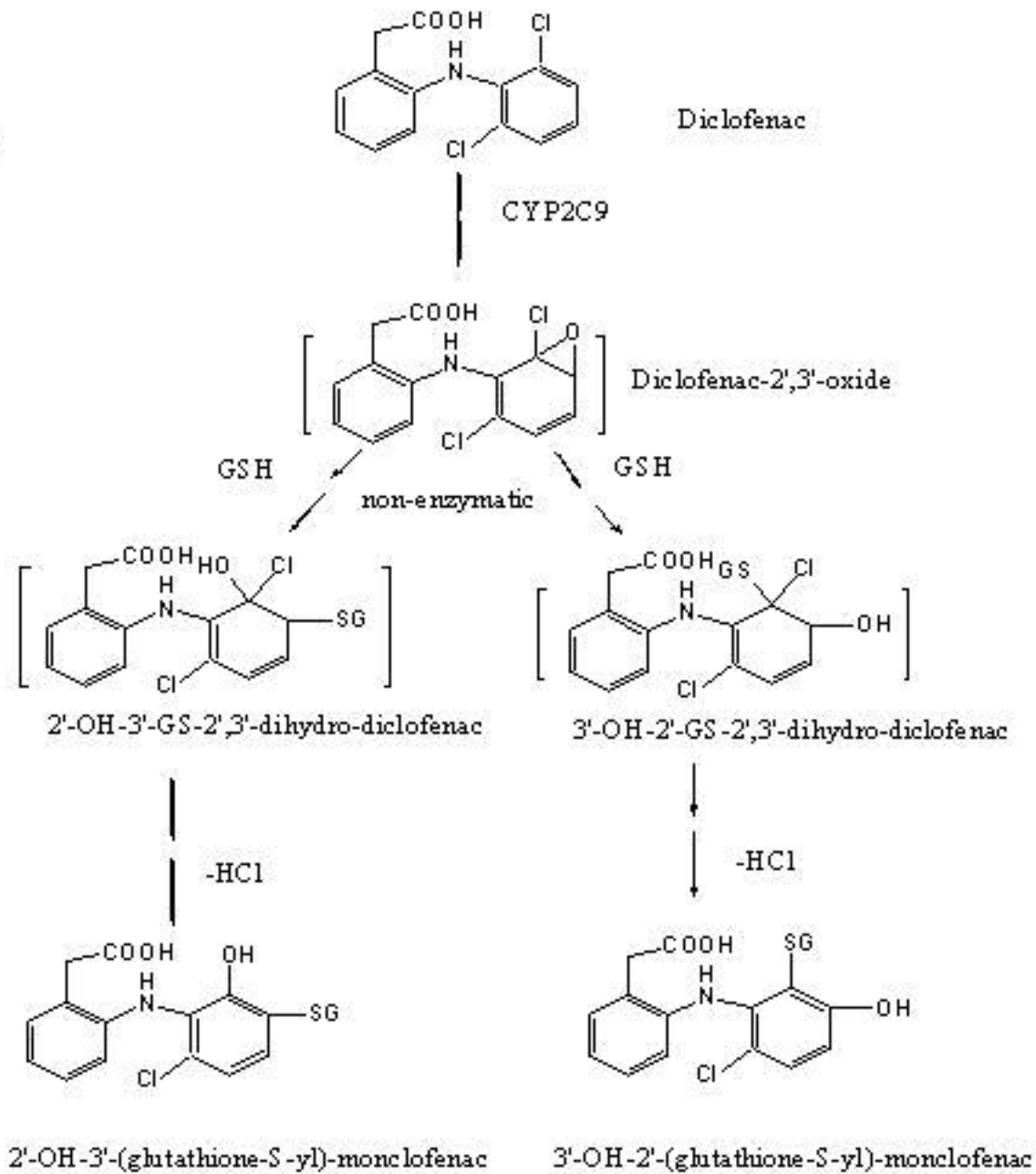
Scheme 1



Scheme 2



Scheme 3.



Scheme 4

